

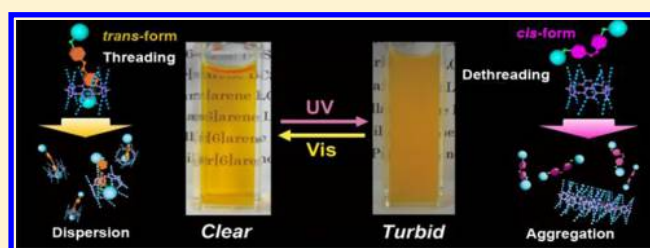
# Photoreversible Switching of the Lower Critical Solution Temperature in a Photoresponsive Host–Guest System of Pillar[6]arene with Triethylene Oxide Substituents and an Azobenzene Derivative

Tomoki Ogoshi,\* Kanako Kida, and Tada-aki Yamagishi

Graduate School of Natural Science and Technology, Kanazawa University, Kakuma-machi, Kanazawa 920-1192, Japan

**S** Supporting Information

**ABSTRACT:** A new water-soluble thermoresponsive pillar[6]arene with triethylene oxide groups was synthesized. The pillar[6]arene showed lower critical solution temperature behavior in aqueous solution. Its clouding point was photoreversibly switched based on a photoresponsive host–guest system. The trans form of an azobenzene guest formed a stable 1:1 complex with the pillar[6]arene. Complexation increased the clouding point. Irradiation with UV light induced a conformation change for the azobenzene guest from the trans to cis form, and dethreading occurred because of a size mismatch between the cis form and the pillar[6]arene cavity. This dethreading decreased the clouding point. The photoresponsive host–guest system was reversible, and the clouding point could be switched by alternating irradiation with UV or visible light. We demonstrated photoresponsive reversible clear-to-turbid and turbid-to-clear transitions for the solution based on the reversible switching of the clouding point using the photosensitive host–guest system.



## INTRODUCTION

Controlling nanoscale supramolecular assemblies by external stimuli is an area of intense interest in nanoscience and nanotechnology. Various external stimuli such as pH,<sup>1</sup> oxidizing and reducing agents,<sup>2</sup> temperature,<sup>3</sup> and light<sup>4</sup> can be used. Among these stimuli, light is especially useful because it works rapidly, remotely, and reversibly and does not generate undesired substances. Azobenzene derivatives are widely used as photoresponsive compounds. Their conformational changes between trans and cis forms with UV or visible light irradiation can be exploited to switch states, for example, between solid and liquid,<sup>4a</sup> sol and gel,<sup>4b–d</sup> and micelle and vesicles.<sup>4e</sup> This can be exploited to trigger shuttling of the wheel segment from one station to another in rotaxanes<sup>4f,g</sup> and supramolecular polymerizations.<sup>4h–j</sup>

Pillararenes, first reported by our group in 2008,<sup>5a</sup> are new macrocyclic hosts bridged at the para-position of the benzene moieties. As a result of their symmetrical pillar architecture and planar chirality,<sup>5e</sup> pillar[5]arene-based supramolecular materials<sup>5g–j</sup> have attracted a great deal of interest. One of the features of pillararenes is their high functionality.<sup>5f–h</sup> Pillararenes have many reactive sites at their rims, and the presence of functional groups at the reactive sites significantly affects their physical properties. We have synthesized a pillar[5]arene with triethylene oxide substituents (Figure 1a, 1).<sup>5j</sup> Pillar[5]arene 1 exhibited lower critical solution temperature (LCST) due to modification of 10 triethylene oxide groups. Interestingly, the clouding point ( $T_{\text{cloud}}$ ) of 1 can be readily adjusted from 42 to

60 °C upon addition of didecylviologen dibromide as a guest. We used cucurbit[7]uril as a competitive host to exclude didecylviologen dibromide from the cavity of 1.  $T_{\text{cloud}}$  was reversed back to that of pristine 1 upon addition of the competitive host. All systems exhibited excellent thermoresponsive properties based on the host–guest system. However, the guest and competitive host added remained in the mixture, which made it difficult to control the LCST reversibility. In this study, light was used to control the LCST. To date, pillararenes with five (pillar[5]arenes) and six (pillar[6]arenes) units have been reported. As compared to pillar[5]arenes, the chemistry of pillar[6]arenes is not as beneficial.<sup>6</sup> The large cavities of pillar[6]arenes should afford new functional supramolecular materials that are not accomplished in pillar[5]arene-based supramolecular materials. In this study, we synthesized a new water-soluble pillar[6]arene with 12 triethylene oxide substituents (Figure 1a, 2) and demonstrated photoreversible switching of the LCST using a photoresponsive host–guest system between the pillar[6]arene 2 and an azobenzene guest (Figure 1b, G1).

## EXPERIMENTAL SECTION

**Materials.** All solvents and reagents were used as supplied. Compound 1 was synthesized according to a previous paper.<sup>5j</sup>

Received: September 13, 2012

Published: November 19, 2012

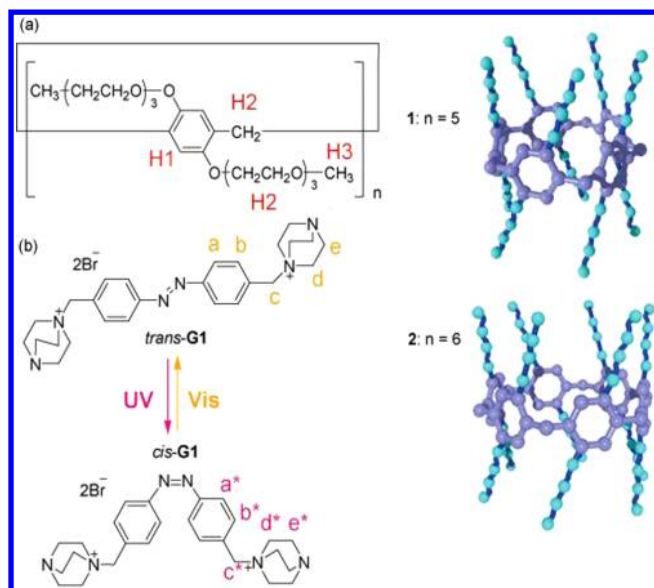


**Figure 1.** Chemical structures of (a) pillar[n]arenes modified with triethylene oxide groups (**1**,  $n = 5$ ; **2**,  $n = 6$ ) and (b) an azobenzene guest (**G1**).

**Measurements.** The  $^1\text{H}$  NMR spectra were recorded at 500 MHz, and  $^{13}\text{C}$  NMR spectra were recorded at 125 MHz with a JEOL-ECA500 spectrometer. UV–vis absorption spectra were recorded with a JASCO V-670. For UV–vis measurements, 1 cm quartz cuvettes were used. Cloud points were determined by transmission changes (at 650 nm) of the solutions heated at  $0.1\text{ }^\circ\text{C}/\text{min}$ ; values of the cloud points were defined as the temperature at which the transmission decreases by 50%.<sup>7</sup>

**2.** *per*-Hydroxylated pillar[6]arene<sup>6d</sup> (100 mg, 0.136 mmol) was dissolved in DMF (2.5 mL) and THF (2.5 mL). Sodium hydride (118 mg, 4.92 mmol) was added, and the reaction mixture was stirred. Next, excess triethylene glycol monomethyl ether mono-*p*-tosylate (1.04 g, 3.27 mmol) was added, and the reaction mixture was heated at  $60\text{ }^\circ\text{C}$  for 96 h. After removal of the solvent, the resulting solid was dissolved in  $\text{CH}_2\text{Cl}_2$ . The organic layer was dried over anhydrous  $\text{Na}_2\text{SO}_4$ . After filtration, the solvent was evaporated to give a solid. Column chromatography (silica gel; dichloromethane:methanol = 96:4) afforded a light yellow liquid (178 mg, 0.0717 mmol, yield: 53%).  $^1\text{H}$  NMR ( $\text{CDCl}_3$ , 500 MHz, ppm):  $\delta$  6.69 (s, 12H, phenyl), 3.92 (t, 24H, methylene), 3.76 (s, 12H, methylene bridge), 3.70 (t, 24H, methylene), 3.67 (t, 24H, methylene), 3.62 (m, 48H, methylene), 3.51 (t, 24H, methylene), 3.34 (s, 36H, methoxy).  $^{13}\text{C}$  NMR ( $\text{CDCl}_3$ , 125 MHz, ppm):  $\delta$  150.6, 128.2, 115.7 (C of phenyl), 72.0, 70.8, 70.7, 70.6, 70.1, 68.4 (C of methylene), 59.0 (C of methyl), 31.1 (C of methylene bridge). LRFABMS:  $m/z$  calcd for  $\text{C}_{126}\text{H}_{205}\text{O}_{48} [\text{M}]^+$ , 2486; found, 2486. HRFABMS:  $m/z$  calcd for  $\text{C}_{126}\text{H}_{205}\text{O}_{48} [\text{M}]^+$ , 2486.3660; found, 2486.3661.

**G1.** To a solution of 4,4'-bis(bromomethyl)azobenzene<sup>8</sup> (500 mg, 1.37 mmol) in acetone (85 mL) was added 1,4-diazabicyclo[2.2.2]octane (920 mg, 8.20 mmol). The solution was stirred at  $50\text{ }^\circ\text{C}$  for 12 h. After the solvent was removed under reduced pressure, the crude was dissolved in methanol. The solution was poured into diethyl ether to reprecipitate the product. The red precipitate was collected by filtration (704 mg, 1.19 mmol, yield: 87%).  $^1\text{H}$  NMR ( $\text{D}_2\text{O}$ , 500 MHz, ppm):  $\delta$  7.93 (d, 4H, phenyl), 7.65 (d, 4H, phenyl), 4.52 (s, 4H, methylene), 3.43 (t, 12H, methylene), 3.11 (t, 12H, methylene).  $^{13}\text{C}$  NMR ( $\text{D}_2\text{O}$ , 125 MHz, ppm):  $\delta$  153.3, 134.4, 129.5, 123.2 (C of phenyl), 67.7, 52.3, 44.3 (C of methylene). LRFABMS:  $m/z$  calcd for  $\text{C}_{26}\text{H}_{36}\text{N}_6 [\text{M} - 2\text{Br}]^{2+}$ , 216; found, 216. HRFABMS:  $m/z$  calcd for  $\text{C}_{26}\text{H}_{36}\text{N}_6 [\text{M} - 2\text{Br}]^{2+}$ , 216.1501; found, 216.1509.

**Determination of the Association Constant.** In the 2-*trans*-G1 complex in  $\text{D}_2\text{O}$ , chemical exchange between free and complexed species is slow on an NMR time scale. Thus,  $^1\text{H}$  NMR spectra of

mixtures of *trans*-G1 and **2** in different ratios showed two sets of resonances for complexed and free *trans*-G1. The association constant  $K$  for 2-*trans*-G1 complex was calculated from integrations of complexed and free signals of the phenyl moiety of *trans*-G1 (Figure 3c, yellow peak b and b').

## RESULTS AND DISCUSSION

**LCST Behavior of 2.** As with **1**,<sup>5j</sup> **2** was soluble in aqueous media and showed LCST behavior. An aqueous solution of **2** at  $25\text{ }^\circ\text{C}$  was clear (Figure 2a) but turbid at  $50\text{ }^\circ\text{C}$  (Figure 2b),

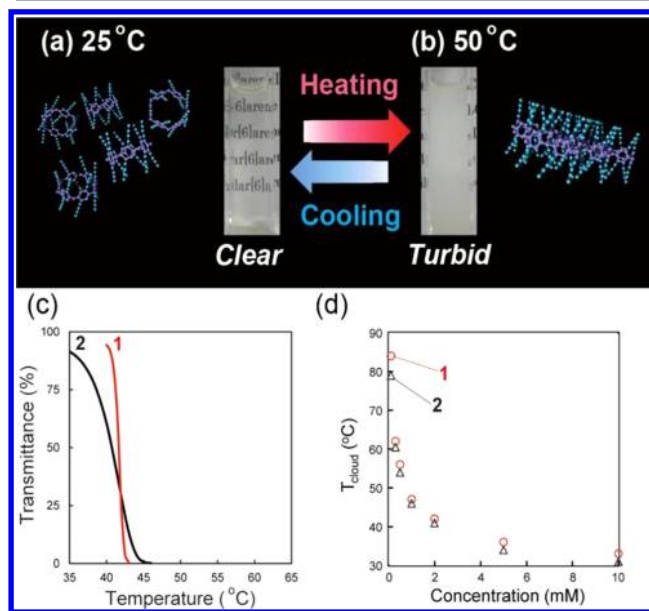


**Figure 2.** Photographs of an aqueous solution containing **2** (2 mM) at (a)  $25\text{ }^\circ\text{C}$  and (b)  $50\text{ }^\circ\text{C}$ . (c) Temperature dependence of light transmittance of **1** (2 mM, red solid line) and **2** (2 mM, black solid line) in aqueous solution. (d) Concentration dependence of the clouding point ( $T_{\text{cloud}}$ ) of **1** and **2** in aqueous solution.

and became clear again when the solution was cooled to  $25\text{ }^\circ\text{C}$ . The LCST behavior of **1** and **2** can be attributed to the interaction of the hydrophobic groups of the pillararene backbone, which results in aggregation and separation from water at temperatures above  $T_{\text{cloud}}$ .  $T_{\text{cloud}}$  was determined by monitoring the change in transmission at 650 nm on a temperature-controlled UV–vis spectrometer (Figure 2c). On heating,  $T_{\text{cloud}}$  of **2** in 2 mM aqueous solution was  $41\text{ }^\circ\text{C}$  (black solid line), which is similar to  $T_{\text{cloud}}$  in **1** ( $42\text{ }^\circ\text{C}$ , red solid line).<sup>5j</sup> Figure 2d shows the effect of concentration on  $T_{\text{cloud}}$ . As the concentration of **1** increased,  $T_{\text{cloud}}$  decreased (red  $\circ$ ), indicating that  $T_{\text{cloud}}$  depended the concentration of **1**. The trend is the same as the other molecules showing  $T_{\text{cloud}}$ .<sup>9a</sup> As the concentration of **2** increased,  $T_{\text{cloud}}$  of **2** also decreased (black  $\triangle$ ), which was the same as those of **1**. Differences between the cyclic pentamer **1** and hexamer structures **2** were therefore independent of  $T_{\text{cloud}}$ .

**Host–Guest Property of *trans*-G1 with **1** and **2**.** The cavity size of pillar[6]arenes is approximately  $7.5\text{ \AA}$ ,<sup>6a</sup> which is larger than that of pillar[5]arenes (approximately  $5.5\text{ \AA}$ ).<sup>5a</sup> Because of their large cavity size as compared to pillar[5]arenes, pillar[6]arenes can bind bulky hydrocarbons. We examined host–guest complexation between pillar[6]arene derivatives and 1,4-diazabicyclo[2.2.2]octane (DABCO) cations in organic media.<sup>6b</sup> The DABCO cation is too large to form complexes

with pillar[5]arene derivatives, but fits in the cavity of pillar[6]arene derivatives. In organic media, the *trans* form of azobenzene can reside in the cavity of pillar[6]arene derivatives, but the *cis* form of azobenzene cannot.<sup>6a</sup> On the basis of these host–guest properties of the pillar[6]arene derivatives in organic media, we designed a new water-soluble guest **G1**, which was an azobenzene derivative with two DABCO cations at each end. Complexation of the *trans* form of the **G1** (*trans*-**G1**) with pillar[5]arene **1** and pillar[6]arene **2** in aqueous media was studied by <sup>1</sup>H NMR (Figure 3a–d). When

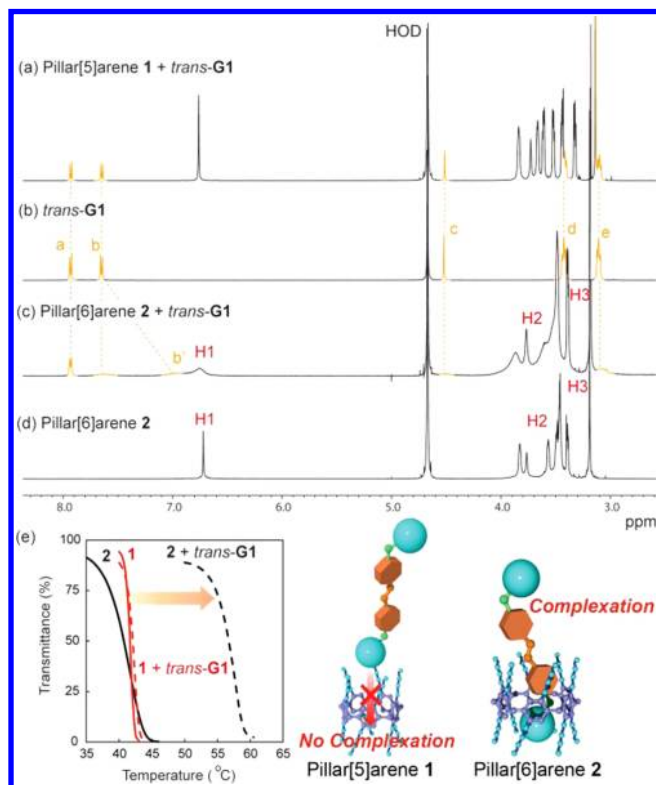


**Figure 3.** <sup>1</sup>H NMR spectra of (a) a mixture of pillar[5]arene **1** and *trans*-**G1**, (b) *trans*-**G1**, (c) a mixture of pillar[6]arene **2** and *trans*-**G1**, and (d) pillar[6]arene **2** in 2 mM in D<sub>2</sub>O. Resonances are labeled in Figure 1. (e) Temperature dependence of light transmittance of **1** (2 mM, red solid line), a mixture of **1** (2 mM) and *trans*-**G1** (8 mM, red dashed line), **2** (2 mM, black solid line), and a mixture of **2** (2 mM) and *trans*-**G1** (8 mM, black dashed line) in aqueous solution.

pillar[5]arene **1** was mixed with *trans*-**G1** in D<sub>2</sub>O, no new peaks or peak shifts were observed for the protons of *trans*-**G1** (yellow peaks, H<sub>a</sub>–H<sub>e</sub>, Figure 3a). This indicates *trans*-**G1** did not form a complex with **1** because pillar[5]arene **1** could not fit over the DABCO cation ends. By contrast, when *trans*-**G1** was mixed with pillar[6]arene **2**, H<sub>b</sub>–H<sub>e</sub> (yellow peaks) proton peaks for *trans*-**G1** and H<sub>1</sub>–H<sub>3</sub> peaks for **2** broadened, while the H<sub>a</sub> proton signal hardly changed (Figure 3c). This indicates that the DABCO cation, methylene, and azobenzene ring containing H<sub>b</sub> were located in the cavity of pillar[6]arene **2**, but the other benzene ring containing H<sub>a</sub> was outside the cavity. An additional peak was observed at about 7 ppm (Figure 3c). The peak was assigned as the complex proton peak H<sub>b</sub><sup>\*</sup> by 2D exchange spectroscopy (Figure S3), and the chemical exchange was slow on the NMR time scale at 25 °C. From the integration ratio of the resonance signals from free (H<sub>b</sub>) and complexed (H<sub>b</sub><sup>\*</sup>) species, the stoichiometry of the **2**-*trans*-**G1** complex

determined from a Job plot was 1:1 (Figure S4), and the association constant (*K*) for the complex was  $(1.01 \pm 0.0031) \times 10^3 \text{ M}^{-1}$  at 25 °C (Figure S5). These results confirm formation of the host–guest complex between **2** and *trans*-**G1**.

**Effect of Host–Guest Complexation between **2** and *trans*-**G1** on *T*<sub>cloud</sub>.** The effect of host–guest complexation on *T*<sub>cloud</sub> was investigated. Upon addition of *trans*-**G1** (8 mM) to **2** (2 mM), *T*<sub>cloud</sub> increased from 41 to 57 °C (Figure 3e, black dashed line). *K* for the complex at *T*<sub>cloud</sub> was obtained by extrapolation using van't Hoff analysis (Figure S5). The extrapolated *K* at *T*<sub>cloud</sub> (57 °C) was high ( $K = (4.81 \pm 0.0029) \times 10^3 \text{ M}^{-1}$ ). The increase in the *T*<sub>cloud</sub> for **2** on addition of *trans*-**G1** is therefore mainly caused by the host–guest complexation. Repulsive forces between the complexed cations might prevent aggregation of **2**. *T*<sub>cloud</sub> did not change when **1** was mixed with *trans*-**G1** (Figure 3e, red dashed line). This is because no complexation occurred between **1** and *trans*-**G1**. The data also support the complexation between *trans*-**G1** and **2**, leading to the observed increase of *T*<sub>cloud</sub>.

**Photoresponsive Host–Guest Complexation System of **2** and **G1**.** Photoisomerization of **G1** in the presence and absence of pillar[6]arene **2** was investigated by <sup>1</sup>H NMR. When the solution containing *trans*-**G1** (Figure 4a) was irradiated

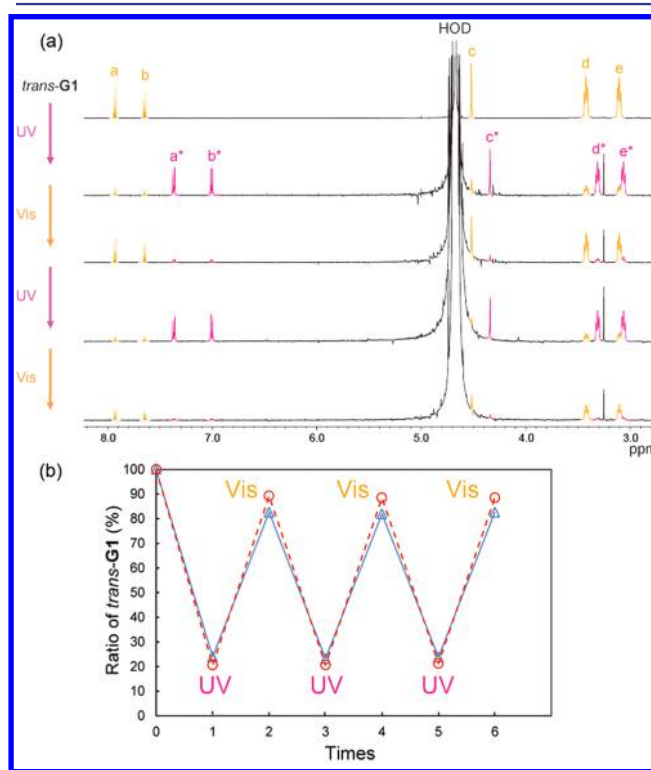


**Figure 4.** (a) <sup>1</sup>H NMR spectra of *trans*-**G1** upon alternating irradiation with UV or visible light in 2 mM in D<sub>2</sub>O at 25 °C. (b) The ratio of *trans*-**G1** in the presence (blue  $\Delta$ ) and absence (red  $\circ$ ) of **2** upon alternating irradiation with UV or visible light in 2 mM in D<sub>2</sub>O at 25 °C.

with UV light (340 nm), new peaks appeared (pink peaks, H<sub>a</sub><sup>\*</sup>–H<sub>e</sub><sup>\*</sup>, Figure 4a). These peaks were assigned to the *cis* form of **G1** (*cis*-**G1**). Yet complete isomerization did not occur. At equilibrium, the *trans*-**G1**/*cis*-**G1** ratio was approximately 21/79, which was determined from the ratio between the proton peaks of H<sub>a</sub> (*trans*-**G1**) and H<sub>a</sub><sup>\*</sup> (*cis*-**G1**). Irradiation of the mixture with visible light (436 nm) allowed recovery of *trans*-



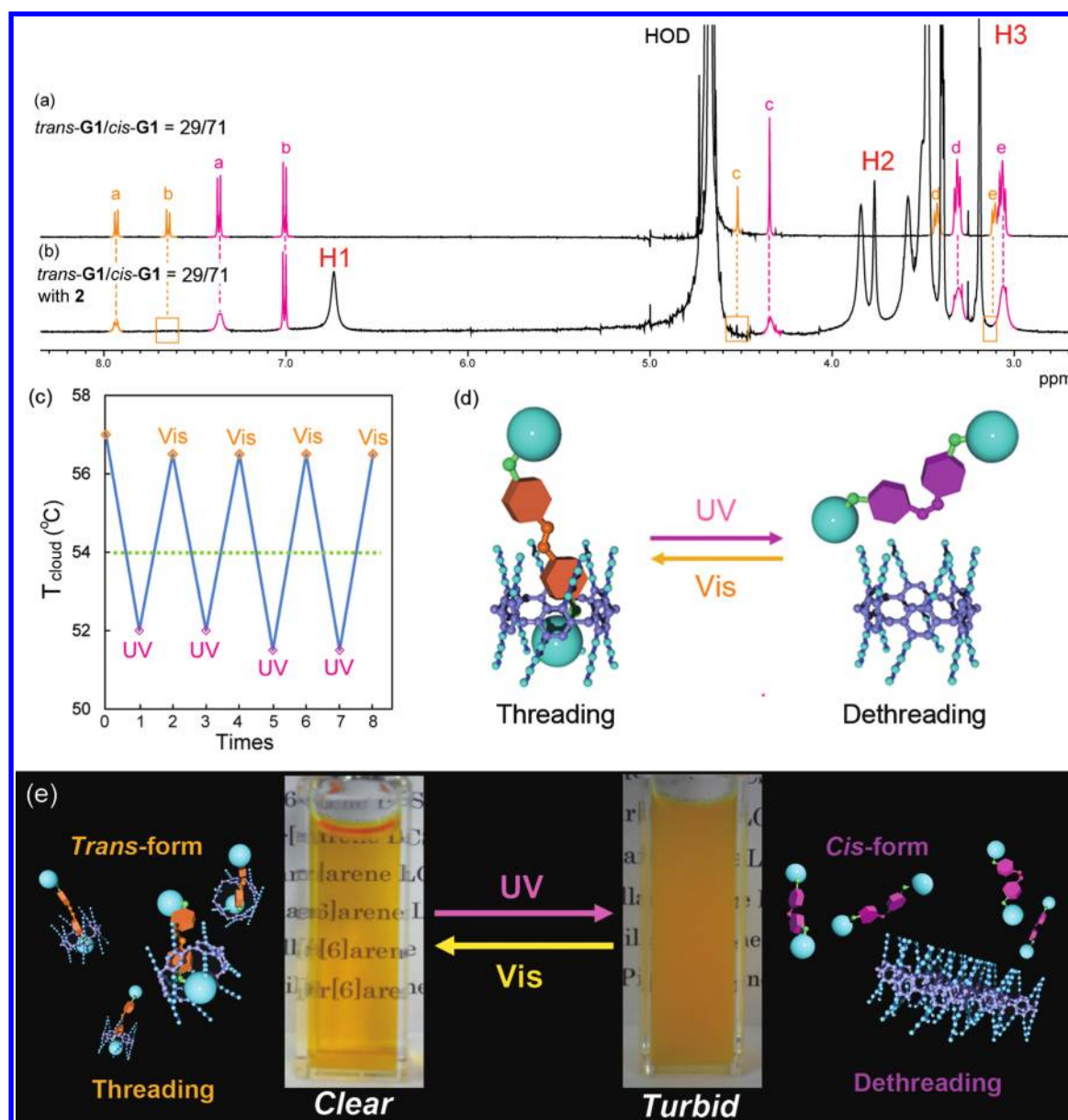


**Figure 5.**  $^1\text{H}$  NMR spectra of a mixture of *trans*-G1 and *cis*-G1 ( $\text{trans-G1}/\text{cis-G1} = 29/71$ ) (b) with and (a) without pillar[6]arene 2. Resonances are labeled in Figure 1. (c) Changes of  $T_{\text{cloud}}$  upon alternating irradiation with UV or visible light. (d) The illustration of photoresponsive host-guest complexation. (e) Photographs for a mixture of 2 (2 mM) and G1 (8 mM) in aqueous solution at 54  $^{\circ}\text{C}$  with alternating UV or visible light irradiation.

G1, but not complete recovery. In the equilibrium state after irradiation with visible light, the *trans*-G1/*cis*-G1 ratio was approximately 89/11. The photoisomerization could be repeated many times (red  $\circ$ , Figure 4b). The reversible photoisomerization was also observed in the presence of 2 (blue  $\triangle$ , Figure 4b). Interaction of pillar[6]arene 2 with *cis*-G1 was examined by  $^1\text{H}$  NMR (Figure 5b). On addition of pillar[6]arene 2 to the solution containing G1 ( $\text{trans-G1}/\text{cis-G1} = 29/71$ ), no peak shifts were observed for the proton signals from *cis*-G1 (pink peaks,  $\text{H}_{\text{a}^*}$ – $\text{H}_{\text{c}^*}$ ). The data indicate no complexation between *cis*-G1 and pillar[6]arene 2. By contrast, the remaining small proton peaks from *trans*-G1 (yellow peaks,  $\text{H}_{\text{b}}$ – $\text{H}_{\text{c}}$ ) broadened. The broadening in Figure 5b was the same as that in Figure 3c. These data indicate that pillar[6]arene 2 can complex with *trans*-G1, but cannot complex with *cis*-G1 (Figure 5d). This is because *trans*-G1 can fit in the cavity of

pillar[6]arene 2, but *cis*-G1 cannot. The photoisomerization from the *trans* to the *cis* form leads to dethreading.

The effect of the threading/dethreading caused by alternating irradiation with UV or visible light on  $T_{\text{cloud}}$  was investigated (Figure 5c). When the host-guest complex of pillar[6]arene 2 and *trans*-G2 was irradiated with UV light (first cycle),  $T_{\text{cloud}}$  decreased from 57 to 52  $^{\circ}\text{C}$ . This is because the photoisomerization from the *trans* to the *cis* form led to dethreading of *cis*-G1 from the cavity of pillar[6]arene 2. After irradiation with visible light (second cycle),  $T_{\text{cloud}}$  increased from 52 to 56.5  $^{\circ}\text{C}$ . Irradiation with visible light caused conversion of *cis*-G1 back to *trans*-G1, and allowed pillar[6]arene 2 complexation with *trans*-G1. The increases and decreases in  $T_{\text{cloud}}$  could be reversibly switched by alternating irradiation with UV or visible light.

On the basis of the reversible switching of  $T_{\text{cloud}}$  using the photosensitive host-guest system, we demonstrated photo-

responsive reversible clear-to-turbid and turbid-to-clear transitions for the solution (Figure 5e). A mixture of pillar[6]arene **2** and *trans*-**G1** was clear at 54 °C because of the  $T_{\text{cloud}}$  of the complex (57 °C). With UV irradiation, the solution at 54 °C changed from clear to turbid because dethreading of *cis*-**G1** from the cavity of pillar[6]arene **2** decreased  $T_{\text{cloud}}$  from 57 to 52 °C. Irradiation with visible light made the 54 °C mixture clear again because *trans*-**G1** from photoisomerization of *cis*-**G1** complexed with pillar[6]arene **2** and increased  $T_{\text{cloud}}$  (56.5 °C). The clear-to-turbid and turbid-to-clear transitions were completely reversible with alternation of UV or visible light irradiation.

## CONCLUSIONS

We demonstrated photoreversible switching of LCST using a photoresponsive host–guest system between a new thermoresponsive macrocyclic host pillar[6]arene **2** and an azobenzene guest **G1** in aqueous media. To the best of our knowledge, this is the first example of photoreversible LCST using a simple host–guest system, although LCST control by combination of poly(*N*-isopropylacrylamide) with a host molecule has been reported.<sup>9</sup> The complexation increased the clouding point. With UV irradiation, the conformation of **G1** changed from the *trans* to *cis* form, and the complex dissociated because of the size mismatch between the *cis* form of **G1** and pillar[6]arene **2**. Visible light irradiation reversed this so the guest could rethread through the host cavity. This photocontrollable threading/dethreading led to photoreversible switching of LCST behavior. All systems in this study exhibited excellent thermoresponsive properties based on the photoresponsive host–guest system. Biocompatible oligoethylene oxide moieties made up a large part of **2**, and the photoreversible switching of LCST was induced with light, which as compared to other external stimuli is relatively clean. Because of these attributes, we believe this system could be used for drug delivery.

## ASSOCIATED CONTENT

### Supporting Information

Characterization data, 2D EXSY, Job plot, and van't Hoff plot. This material is available free of charge via the Internet at <http://pubs.acs.org>.

## AUTHOR INFORMATION

### Corresponding Author

ogoshi@t.kanazawa-u.ac.jp

### Notes

The authors declare no competing financial interest.

## ACKNOWLEDGMENTS

This work was partly supported by the Nanotechnology Platform Program of the Ministry of Education, Culture, Sports, Science, and Technology (MEXT), Japan, and JSPS KAKENHI 23655210 (a Grant-in-Aid for Challenging Exploratory Research).

## REFERENCES

(1) (a) Badjic, J. D.; Balzani, V.; Credi, A.; Silvi, S.; Stoddart, J. F. *Science* **2004**, *303*, 1845–1849. (b) Ashton, P. R.; Ballardini, R.; Balzani, V.; Gomez-Lopez, M.; Lawrence, S. E.; Martinez-Diaz, M. V.; Montalti, M.; Piersanti, A.; Prodi, L.; Stoddart, J. F.; Williams, D. J. *J. Am. Chem. Soc.* **1997**, *119*, 10641–10651. (c) Suzuki, S.; Nakazono, K.; Takata, T. *Org. Lett.* **2010**, *12*, 712–715. (d) Lee, M.; Lee, S. J.; Jiang, L. H. *J. Am. Chem. Soc.* **2004**, *126*, 12724–12725.

(2) Fahrenbach, A. C.; Bruns, C. J.; Cao, D.; Stoddart, J. F. *Acc. Chem. Res.* **2012**, *45*, 1581–1592.

(3) (a) Umehara, T.; Kawai, H.; Fujiwara, K.; Suzuki, T. *J. Am. Chem. Soc.* **2008**, *130*, 13981–13988. (b) Ogoshi, T.; Yamafuji, D.; Aoki, T.; Yamagishi, T. *Chem. Commun.* **2012**, *48*, 6842–6844.

(4) (a) Akiyama, H.; Yoshida, M. *Adv. Mater.* **2012**, *24*, 2353–2356. (b) Rajaganesh, R.; Gopal, A.; Das, T. M.; Ajayaghosh, A. *Org. Lett.* **2012**, *14*, 748–751. (c) Suzuki, T.; Shinkai, S.; Sada, K. *Adv. Mater.* **2006**, *18*, 1043–1046. (d) Tomatsu, I.; Hashidzume, A.; Harada, A. *Macromolecules* **2005**, *38*, 5223–5227. (e) Yang, L. L. Y.; Dong, J.; Li, X. *J. Colloid Interface Sci.* **2010**, *343*, 504–509. (f) Inoue, Y.; Kuad, P.; Okumura, Y.; Takashima, Y.; Yamaguchi, H.; Harada, A. *J. Am. Chem. Soc.* **2007**, *129*, 6396–6397. (g) Coskun, A.; Friedman, D. C.; Li, H.; Patel, K.; Khatib, H. A.; Stoddart, J. F. *J. Am. Chem. Soc.* **2009**, *131*, 2493–2495. (h) Lohmann, F.; Ackermann, D.; Famulok, M. *J. Am. Chem. Soc.* **2012**, *134*, 11884–11887. (i) Yamauchi, K.; Takashima, Y.; Hashidzume, A.; Yamaguchi, H.; Harada, A. *J. Am. Chem. Soc.* **2008**, *130*, 5024–5025. (j) Kuad, P.; Miyawaki, A.; Takashima, Y.; Yamaguchi, H.; Harada, A. *J. Am. Chem. Soc.* **2007**, *129*, 12630–12631.

(5) (a) Ogoshi, T.; Kanai, S.; Fujinami, S.; Yamagishi, T.; Nakamoto, Y. *J. Am. Chem. Soc.* **2008**, *130*, 5022–5023. (b) Ogoshi, T. *J. Inclusion Phenom. Macrocyclic Chem.* **2012**, *72*, 247–262. (c) Cragg, P. J.; Sharma, S. *Chem. Soc. Rev.* **2012**, *41*, 597–607. (d) Xue, M.; Yang, Y.; Chi, X.; Zhang, Z.; Huang, F. *Acc. Chem. Res.* **2012**, *45*, 1294–1308. (e) Ogoshi, T.; Masaki, K.; Shiga, R.; Kitajima, K.; Yamagishi, T. *Org. Lett.* **2011**, *13*, 1264–1266. (f) Ogoshi, T.; Shiga, R.; Hashizume, M.; Yamagishi, T. *Chem. Commun.* **2011**, *47*, 6927–6929. (g) Strutt, N. L.; Forgan, R. S.; Spruell, J. M.; Botros, Y. Y.; Stoddart, J. F. *J. Am. Chem. Soc.* **2011**, *133*, 5668–5671. (h) Strutt, N. L.; Zhang, H.; Giesener, M. A.; Lei, J.; Stoddart, J. F. *Chem. Commun.* **2012**, *48*, 1647–1649. (i) Ogoshi, T.; Yamafuji, D.; Aoki, T.; Kitajima, K.; Yamagishi, T.; Hayashi, Y.; Kawachi, S. *Chem.-Eur. J.* **2012**, *18*, 7493–7500. (j) Ogoshi, T.; Shiga, R.; Yamagishi, T. *J. Am. Chem. Soc.* **2012**, *134*, 4577–4580.

(6) (a) Yu, G.; Han, C.; Zhang, Z.; Chen, J.; Yan, X.; Zheng, B.; Liu, S.; Huang, F. *J. Am. Chem. Soc.* **2012**, *134*, 8711–8717. (b) Ogoshi, T.; Kayama, H.; Yamafuji, D.; Aoki, T.; Yamagishi, T. *Chem. Soc.* **2012**, *3*, 3221–3226. (c) Ogoshi, T.; Yamafuji, D.; Aoki, T.; Yamagishi, T. *Chem. Commun.* **2012**, *48*, 6842–6844. (d) Ma, Y.; Chi, X.; Yan, X.; Liu, J.; Yao, Y.; Chen, W.; Huang, F.; Hou, J. L. *Org. Lett.* **2012**, *14*, 1532–1535.

(7) Munteanu, M.; Choi, S. W.; Ritter, H. *Macromolecules* **2009**, *42*, 3887–3891.

(8) Qipeng, G.; Zhikai, Z. *Mater. Sci. Eng., C* **2000**, *7*, 91–98.

(9) (a) Afroze, F.; Nies, E.; Berghmans, H. *J. Mol. Struct.* **2000**, *554*, 55–68. (b) Ogoshi, T.; Masuda, K.; Yamagishi, T.; Nakamoto, Y. *Macromolecules* **2009**, *42*, 8003–8005. (c) Yhaya, F.; Lim, J.; Kim, Y.; Liang, M.; Gregory, A. M.; Stenzel, M. H. *Macromolecules* **2011**, *44*, 8433–8445. (d) Sambe, L. N.; Stoffelbach, F. O.; Lyskawa, J.; Delattre, F. O.; Fournier, D.; Bouteiller, L.; Charleux, B.; Cooke, G.; Woisel, P. *Macromolecules* **2011**, *44*, 6532–6538. (e) Bigot, J.; Charleux, B.; Cooke, G.; Delattre, F. O.; Fournier, D.; Lyskawa, J. I.; Sambe, L. N.; Stoffelbach, F. O.; Woisel, P. *J. Am. Chem. Soc.* **2010**, *132*, 10796–10801. (f) Amajjahe, S.; Ritter, H. *Macromolecules* **2008**, *41*, 3250–3253. (g) Koopmans, C.; Ritter, H. *J. Am. Chem. Soc.* **2007**, *129*, 3502–3503. (h) Plamper, F. A.; Schmalz, A.; Ballauff, M.; Müller, A. H. E. *J. Am. Chem. Soc.* **2007**, *129*, 14538–14539. (i) Mao, H.; Li, C.; Zhang, Y.; Bergbreiter, D. E.; Cremer, P. S. *J. Am. Chem. Soc.* **2005**, *125*, 2850–2851. (j) Klaukherd, A.; Nagamini, C.; Thayumanavan, S. *J. Am. Chem. Soc.* **2009**, *131*, 4830–4838.